# Temperature dependence of the pressure-induced amorphization of ice $I_h$ studied by high-pressure neutron diffraction to 30 K

Thierry Strässle,* Andrin Caviezel,† Balasubramanian Padmanabhan, and Vladimir Yu. Pomjakushin
*Laboratory for Neutron Scattering, ETH Zurich and Paul Scherrer Institut, 5232 Villigen PSI, Switzerland*

Stefan Klotz
*IMPMC, CNRS-UMR 7590, Université Pierre & Marie Curie, 75252 Paris, France*
(Received 14 March 2010; revised manuscript received 2 July 2010; published 13 September 2010)

High-pressure neutron diffraction allowed the *in situ* observation of the pressure-induced amorphization of ordinary ice $I_h$ between 130 and 30 K, i.e., to lower temperatures than any other diffraction study before. We find that the pressure required for complete transformation into high-density amorphous ice (HDA) increases with decreasing temperature to ~80 K but remains approximately constant below. Our findings support earlier evidence of two distinct mechanisms responsible for the pressure-induced amorphization in ice $I_h$, namely, amorphization due to mechanical melting down to lowest temperatures, and amorphization due to thermal melting at elevated temperatures. Such scenario naturally explains why HDA prepared through compression at 77 K is structurally distinct from the form of HDA obtained by the compression of low-density amorphous ice (LDA) and hence cannot be associated with the hypothesized high-density proxy of liquid water in a two-state model.

DOI: 10.1103/PhysRevB.82.094103 PACS number(s): 61.05.F−, 62.50.−p, 31.70.Ks, 61.43.Er

## I. INTRODUCTION

The ordinary form of ice, phase $I_h$, exhibits solid-state amorphization (SSA) when compressed at low temperatures. Ice $I_h$ serves as a textbook example for complete SSA, despite the fact that SSA has been identified in many more materials[1] after the discovery in ice $I_h$ by Mishima *et al.* in 1984,[2] and despite the fact that pressure-induced SSA has been reported as early as 1972 for $Gd_2(MoO_4)_3$ by Brixner.[3] Many of these materials are common minerals and hence their SSA behavior is of direct relevance for geophysics. A well-known feature of most of these systems are a negative melting line and a negative thermal expansion coefficient at low temperatures. Both properties are intimately connected to peculiarities in the vibrational properties of the crystalline phase and require low-energy phonon modes with negative Grüneisen parameters.[4] In spite of many theoretical and experimental efforts no consensus has been found on what general mechanism leads to SSA in these materials. Part of the difficulties relates to the fact that the amorphous state itself often remains ill-defined. This leads, for example, to the odd terminology of *Raman amorphous* or *x-ray amorphous* depending on the experimental method used to characterize the amorphous product (Ref. 1 and references therein). There is also the well-known difficulty in unambiguously differentiating between amorphous and nanocrystalline forms of matter.

Ice is without doubt the clearest example of a solid showing pressure-induced amorphization. The amorphization of ice $I_h$ is easily probed by, e.g., Raman spectroscopy of the O-H stretching mode or by diffraction. Both methods give the same picture of a complete loss of crystallinity in ice $I_h$ when sufficiently compressed at temperatures below 130 K. The truly disordered nature of the high-pressure product is further supported by the existence of a glass transition.[5,6] For this reason ice is unquestionable the ideal case to study the mechanisms leading to pressure-induced amorphization.

In this study we have employed *in situ* high-pressure neutron diffraction on deuterated ice $I_h$ and studied the process of amorphization with increasing pressure at different temperatures. To the best of our knowledge, *in situ* Raman or diffraction measurements on the amorphization of ice have not been reported for temperatures below 77 K thus leaving room for speculation. Our results show that ice $I_h$ can still be amorphized at 30 K however due to a different mechanism than effective at higher temperatures.

## II. EXPERIMENTAL

A sample of 70 $mm^3$ liquid $D_2O$ was loaded into a titanium-zirconium encapsulating gasket assembly and compressed with a pneumatically driven VX5 Paris-Edinburgh press employing boron-nitride opposed anvils. A helium gas pressure of 15 bar on the piston of the press corresponds to a nominal force of 10 kN on the gasket-sample assembly. Details of the low-temperature setup can be found elsewhere.[7,8] A small piece of lead added to the sample served as a pressure calibrant via its known equation of state (EOS) corrected for thermal expansion.[9] The sample was rapidly cooled in order to avoid the formation of single crystals and to assure a reasonably polycrystalline ice $I_h$ sample to start amorphization with. Diffraction patterns were collected on the powder diffractometer HRPT[10] at the continuous spallation neutron source SINQ of the Paul Scherrer Institute in Villigen (Switzerland) using a neutron wavelength of 1.886 Å. Five isothermal runs at $T=30$, 55, 80, 105, and 130 K were recorded.

## III. RESULTS

Figures 1 and 2 show representative diffraction patterns for the amorphization at 130 K and 30 K, respectively. Full

 

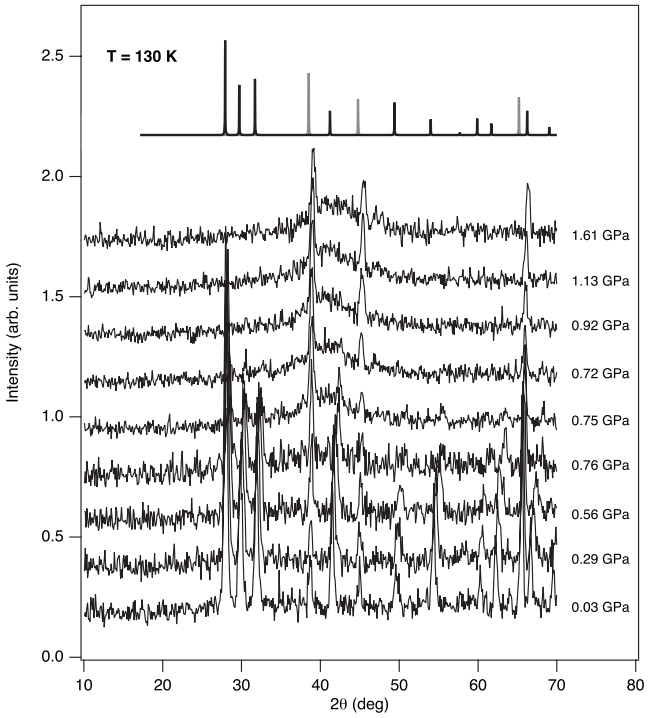


FIG. 1. Neutron-diffraction patterns showing the gradual transformation from ice $I_h$ to HDA with increasing pressure at $T=130$ K. Upper figure: calculated peak positions for ice $I_h$ (black) and Pb (gray).

amorphization of the sample is characterized by a complete disappearance of all Bragg peaks of crystalline ice $I_h$ and the occurrence of a broad feature at about $2\theta=40°$ ($Q$

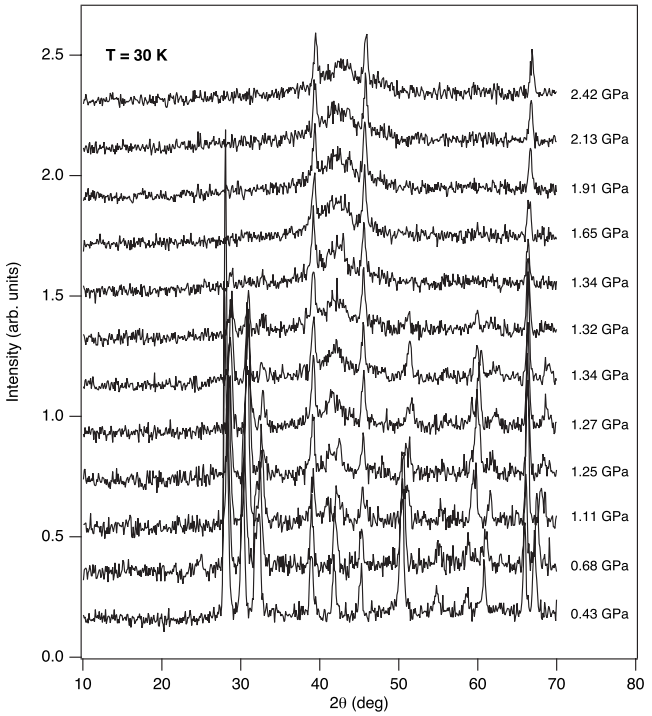


FIG. 2. Neutron-diffraction patterns showing the transformation from ice $I_h$ to HDA with increasing pressure at $T=30$ K.

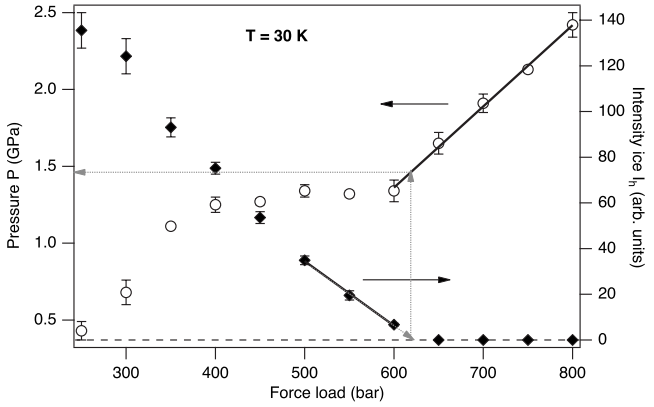


FIG. 3. Representative figure illustrating the determination of the pressure value for full amorphization $P_c$. Open symbols (left axis) show pressure values determined from the Pb calibrant as a function of load acting on the sample (details see text). Solid symbols (right axis) show the sum of integrated intensities of the 100, 002, and 101 Bragg reflections of ice $I_h$. The load where the intensity of ice $I_h$ vanishes is extrapolated and corresponding pressure $P_c$ interpolated (details see text).

$\sim 2.4$ Å$^{-1}$). The remaining Bragg peaks are due to the pressure calibrant (Pb). Inspection of Figs. 1 and 2 already indicates that for full amorphization at $T=30$ K considerably higher pressures are needed than at $T=130$ K. In order to quantify and compare pressures required for complete amorphization of ice $I_h$ at different $T$, Bragg intensities of ice $I_h$ are monitored as a function of applied load and resulting pressure. Figure 3 shows the summed intensity of the 100, 002, and 101 triplet of Bragg peaks characteristic of ice $I_h$ together with the corresponding pressure determined from the position of the Pb peaks as a function of load $F$. With increasing $F$ the intensity of the ice $I_h$ Bragg peaks decreases. In the beginning ($F \lesssim 400$ bar) the decrease in the scattering signal is dominated by large initial compression of the sample-gasket assembly and resulting closure of the anvils. In addition the pressure-induced development of preferred grain orientation in the powder sample may influence the Bragg intensities more strongly at lower loads than at high load where a certain preferred orientation already has been established. The amorphization itself is visible as a plateau in the measured pressure $P(F)$ as a function of load. We note here that inherent to our high-pressure technique, the applied load essentially controls the volume available to the sample. The plateau in $P(F)$ hence naturally reflects the characteristics of a first-order transition where the fraction of the low-density phase (ice $I_h$) gradually reduces with decreasing sample volume at constant pressure, in favor of the high-pressure phase [high-density amorphous ice (HDA)], until the sample has entirely transformed. The load value $F_c$ for full amorphization of the sample has been determined from extrapolation of the last few Bragg intensities of ice $I_h$ within the plateau, i.e., transition region. The corresponding critical pressure is then mapped by interpolation of $P(F \searrow F_c)$. Obviously, $F_c$ is found at values slightly to the right of the plateau, i.e., in a region where the pressure vs load relation $P(F)$ adopts a linear dependence again. Figure 4 shows the last three diffraction patterns before and one right after full

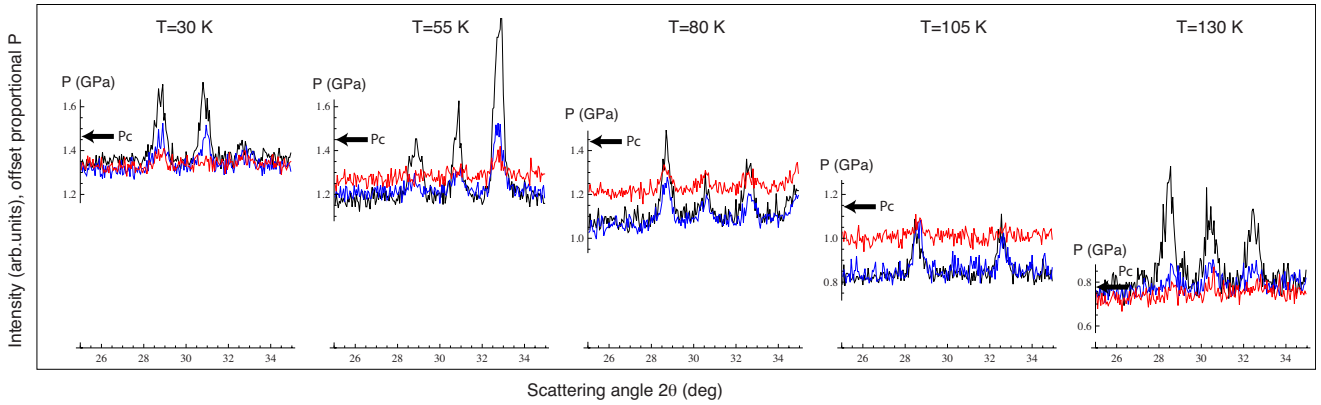


FIG. 4. (Color online) Neutron-diffraction patterns with the 100, 002, and 101 reflections of ice $I_h$ measured at subsequent load increments for five different temperatures. The samples exhibit preferred orientations as seen by the varying ratio of peak intensities. The individual patterns are shifted along the $y$ axis proportionally to the pressures they were measured at. Values of $P_c$ determined by the procedure exemplified in Fig. 3 are shown as arrows.

amorphization, respectively, each shifted with a vertical offset corresponding to the measured pressure value. Patterns at full amorphization are displaced nonequidistantly due to the steep increase in $P$ after the plateau. Already qualitative inspection of Fig. 4 reveals a smaller temperature dependence of $P_c$ between $T=30$, 55, and 80 K than between $T=80$, 105, and 130 K. Quantitative values of $P_c$ determined by the above described method (see Fig. 3) are included as arrows in Fig. 4 and summarized in Fig. 5 underpinning a change in the temperature dependence of $P_c$ at around 80 K. The values of $P_c$ found here are in good agreement to reported pressures[2,11–13] for full amorphization at liquid nitrogen temperature ($T\sim 77$ K) and above.

## IV. DISCUSSION

The main observation made in this study, namely, that the pressure required for complete transformation into HDA increases with decreasing temperature to ~80 K, but remains approximately constant below, is strong experimental evidence of a scenario where two distinct mechanisms are responsible for SSA in ice $I_h$.[8] Already in the first report of SSA in ice $I_h$, Mishima *et al.*[2,11] conjectured that amorphization of ice arises due to *thermal melting* by pointing out that the extrapolated melting line approximately matches the observed values of $P_c$. In a microscopic picture this mechanism is rationalized with the Lindemann criterion stating that a solid melts if thermal atomic (or molecular) displacements exceed an empirical fraction of the interatomic (intermolecular) distances.[14,15] Shortly thereafter, Tse *et al.*[16,17] proposed another mechanism responsible for the observed amorphization. Herein, amorphization arises due to a violation of Born's criteria requiring the elastic tensor always to be positive definite.[18] In a microscopic picture this so-called *mechanical melting* is equivalent to a complete softening of some of the acoustic phonon branches near the center of the Brillouin zone. More generally, it has been proposed that lattice instabilities associated with a dispersionless complete softening of one or more acoustic phonon branches results in mechanical melting since a manifold of phonon wave vectors approach zero frequency simultaneously and hence provoke a manifold of inhibited frustrated structural transitions.[19]

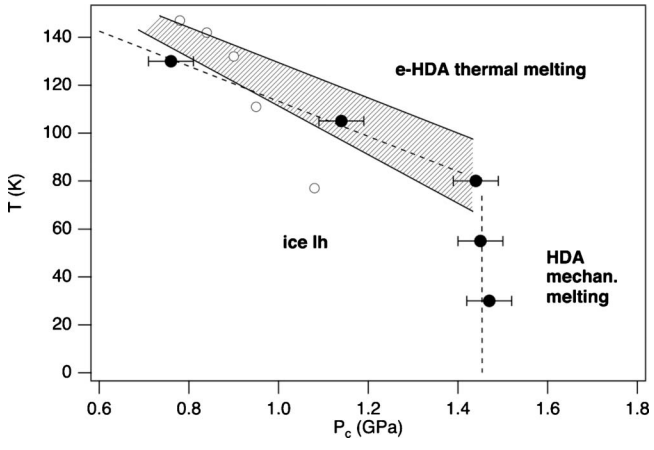


FIG. 5. Pressures $P_c$ for complete amorphization of ice $I_h$ as a function of temperature (solid circles, this work). The shaded region depicts estimated pressures for close-to-complete (>90%) amorphization deduced from Ref. 11 (Fig. 1) and Ref. 2 (Fig. 1), open circles refer to corresponding "nominal pressure" values for the onset of amorphization from Ref. 11 [Fig. 2(a)].

The pressure dependence of the phonon dispersion of ice $I_h$ has been determined in a previous study and the phonon branches exhibiting pronounced softening have been identified by neutron scattering,[4] giving values which are consistent with macroscopic measurements of Grüneisen parameters.[20] The softening naturally explains on a quantitative level the negative melting line and the known negative thermal expansion below $T\approx 70$ K of ice $I_h$. With the mode Grüneisen parameters at hand pressures for both the violation of the criteria of Lindemann $P_c^L(T)$ and Born $P_c^B(T)$, responsible for thermal and mechanical melting, respectively, could be calculated.[8] Since both criteria define upper limits for the crystalline phase to sustain, $P_c^L(T)$ and $P_c^B(T)$ must be compared to the observed experimental values $P_c(T)$ for complete transformation into the amorphous phase and not to the onset of amorphization. Latter depends on the local and microscopic stress distribution of the sample and hence may

show a dependency on the sample preparation and pressure apparatus. Evidence of a dependence upon grain size of the sample has been indeed reported by Johari.[21]

## V. CONCLUSION AND SUMMARY

We now briefly summarize the expected temperature dependence of the two criteria for amorphization (see Ref. 8 for a detailed discussion) and compare it with the observed values of pressure for full amorphization. In first approximation, temperature-independent pressure-induced effects on the phonon dispersion (i.e., temperature-independent mode Grüneisen parameters) may be assumed. It then follows that $P_c^B(T) \equiv$ const independent on $T$ whereas $P_c^L(T)$ is a function of $T$ due to the thermal activated nature of molecular displacements. The two calculated transition lines are found to cross near $T=80$ K and $P=1.3$ GPa.[8] The experimentally observed upper critical pressures $P_c(T)$ for complete amorphization in ice $I_h$ presented here are in excellent agreement with this scenario of a crossover between two distinct amorphization mechanisms. This scenario also naturally explains two experimental observations well known to HDA formed by compression of ice $I_h$ at liquid nitrogen temperature (77 K). First, this form of HDA, also referred as to u-HDA (Ref. 22) is different from the form of HDA obtained from compression of low-density amorphous ice (LDA) (Refs. 12 and 23) since it resulted dominantly via mechanical melting and hence per se contains inherent structural defects that are remnants of the inhibited frustrated phase transitions. Indeed, u-HDA has been shown to transform toward a relaxed from of HDA at $T>80$ K, referred to as e-HDA,[22] while kept at sufficiently small pressures in order to inhibit transformation into LDA, whereas at lower $T$ u-HDA remains stable.[22] Second, if amorphized at 130 K$>T\gg 80$ K the amorphous product is equivalent to e-HDA since it resulted via thermal melting and hence per se is a relaxed phase free of local defects. It is this form of HDA, i.e., e-HDA, that might be considered as the amorphous proxy of the high-density form of water relevant for the scenario of a second critical point in the phase diagram of water.

## ACKNOWLEDGMENTS

The excellent technical assistance of Walter Latscha, Markus Zolliker, and Stephan Fischer is gratefully acknowledged. We thank Karl Syassen, Clemens Ulrich, and Uwe Engelhardt (MPI Stuttgart) for providing us the gas compressor system used in these measurements. This work is based on experiments performed at the Swiss spallation neutron source SINQ, Paul Scherrer Institute, Villigen, Switzerland.

*thierry.straessle@psi.ch
†Also at the Swiss Light Source, Paul Scherrer Institut, 5232 Villigen PSI, Switzerland.

[1] S. M. Sharma and S. K. Sikka, Prog. Mater. Sci. **40**, 1 (1996).
[2] O. Mishima, L. D. Calvert, and E. Whalley, Nature (London) **310**, 393 (1984).
[3] L. H. Brixner, Mater. Res. Bull. **7**, 879 (1972).
[4] T. Strässle, A. M. Saitta, S. Klotz, and M. Braden, Phys. Rev. Lett. **93**, 225901 (2004).
[5] O. Andersson, Phys. Rev. Lett. **95**, 205503 (2005).
[6] M. Seidl, T. Loerting, and G. Zifferer, J. Chem. Phys. **131**, 114502 (2009).
[7] S. Klotz, B. Padmanabhan, J. Philippe, and T. Strässle, High Press. Res. **28**, 621 (2008).
[8] T. Strässle, S. Klotz, G. Hamel, M. M. Koza, and H. Schober, Phys. Rev. Lett. **99**, 175501 (2007).
[9] Birch-Murnaghan EOS of Pb at 85 K: $B=44.8$ GPa and $B'=5.5$, derived from EOS at 300 K using Vinet's Eq. (4.5) (Ref. 24) and known thermal expansion (Ref. 25). Room-temperature EOS ($B=41.2$ GPa, $B'=5.5$) established via EOS of NaCl (Ref. 26) in separate run. $\Delta V/V$ corrected for thermal expansion (Ref. 25) to $T=85$ K. Within 30 K$\leq T\leq$130 K, $B$ varies by less than $\pm 2\%$ from the value at 85 K.
[10] P. Fischer *et al.*, Physica B **276-278**, 146 (2000).
[11] O. Mishima, Nature (London) **384**, 546 (1996).
[12] O. Mishima, J. Chem. Phys. **100**, 5910 (1994).
[13] R. Martoňák, D. Donadio, and M. Parrinello, Phys. Rev. Lett. **92**, 225702 (2004).
[14] F. A. Lindemann, Z. Phys. **11**, 609 (1910).
[15] J. J. Gilvarry, Phys. Rev. **102**, 308 (1956).
[16] J. S. Tse, J. Chem. Phys. **96**, 5482 (1992).
[17] J. S. Tse, D. D. Klug, C. A. Tulk, I. Swainson, E. C. Svensson, C. K. Loong, V. Shpakov, V. R. Belosludov, R. V. Belosludov, and Y. Kawazoe, Nature (London) **400**, 647 (1999).
[18] M. Born and K. Huang, *Dynamical Theory of Crystal Lattices* (Clarendon, Oxford, 1954).
[19] M. H. Cohen, J. Iniguez, and J. B. Neaton, J. Non-Cryst. Solids **307-310**, 602 (2002).
[20] O. Andersson and A. Inaba, J. Chem. Phys. **122**, 124710 (2005).
[21] G. P. Johari, Phys. Chem. Chem. Phys. **2**, 1567 (2000).
[22] R. J. Nelmes, J. S. Loveday, T. Strässle, C. L. Bull, M. Guthrie, G. Hamel, and S. Klotz, Nat. Phys. **2**, 414 (2006).
[23] S. Klotz, T. Strässle, G. Hamel, R. J. Nelmes, J. S. Loveday, G. Rousse, B. Canny, J. C. Chervin, and A. M. Saitta, Phys. Rev. Lett. **94**, 025506 (2005).
[24] P. Vinet, J. R. Smith, J. Ferrante, and J. H. Rose, Phys. Rev. B **35**, 1945 (1987).
[25] T. Rubin, H. L. Johnston, and H. W. Altman, J. Phys. Chem. **66**, 266 (1962).
[26] J. M. Brown, J. Appl. Phys. **86**, 5801 (1999).